

Full paper / Mémoire

Cobalt supported on alumina and silica-doped alumina: Catalyst structure and catalytic performance in Fischer–Tropsch synthesis

Alan Jean-Marie^{a,b}, Anne Griboval-Constant^{a,*}, Andrei Y. Khodakov^{a,*},
Fabrice Diehl^b

^a *Unité de catalyse et de chimie du solide, Université des sciences et technologies de Lille, UMR CNRS 8181, USTL-ENSCL-EC Lille, bâtiment C3, Cité scientifique, 59655 Villeneuve d'Ascq, France*

^b *IFP-Lyon, BP 3, 69360 Solaize cedex, France*

Received 28 April 2008; accepted after revision 16 July 2008

Available online 26 February 2009

Abstract

The paper addresses the structure and catalytic performance in fixed bed reactor at 20 bars of cobalt Fischer–Tropsch catalysts supported by commercial alumina (Puralox) and silica-doped alumina (Siralox). The cobalt loading varied between 8 and 15 wt.%; both alumina and silica-doped alumina supports had similar textural properties. Cobalt dispersion in both supports was principally affected by support pore diameter; at high cobalt loadings, cobalt particle size slightly increased with cobalt content. The presence of small amounts of silica in alumina (5 wt.% SiO₂) enhanced cobalt reducibility and hindered formation of hardly reducible cobalt aluminate species. Higher Fischer–Tropsch reaction rate over cobalt catalysts supported on silica-doped alumina was attributed to a better cobalt reducibility. **To cite this article:** A. Jean-Marie et al., C. R. Chimie 12 (2009).

© 2009 Académie des sciences. Published by Elsevier Masson SAS. All rights reserved.

Résumé

Cet article porte sur la structure et les performances catalytiques dans un réacteur à lit fixe des catalyseurs Fischer–Tropsch à base de cobalt supportés par alumine (Puralox) ou par alumine dopée au silicium (Siralox). Le taux de cobalt varie entre 8 et 15% en poids; les deux supports présentent des caractéristiques texturales proches. Il a été constaté que la dispersion du cobalt était principalement influencée par le diamètre des pores. Par ailleurs, à des teneurs élevées en cobalt, la taille des particules d'oxyde de cobalt tend à augmenter légèrement avec la teneur en métal. La présence de silice dans l'alumine (5% poids de SiO₂) améliorerait la réductibilité du cobalt et empêcherait la formation de phases d'aluminate de cobalt inactives en synthèse Fischer–Tropsch. Les catalyseurs qui contiennent de la silice ont montré une vitesse de réaction plus importante. Ceci a été attribué à une meilleure réductibilité du cobalt. **Pour citer cet article :** A. Jean-Marie et al., C. R. Chimie 12 (2009).

© 2009 Académie des sciences. Published by Elsevier Masson SAS. All rights reserved.

Keywords: Clean fuels; Fischer–Tropsch synthesis; Cobalt catalysts; Catalyst support; Nanoparticles

Mots-clés : Carburants propres ; Synthèse Fischer–Tropsch ; Catalyseur cobalt ; Support catalytique ; Nanoparticules

* Corresponding authors.

E-mail addresses: anne.griboval@univ-lille1.fr (A. Griboval-Constant), andrei.khodakov@univ-lille1.fr (A.Y. Khodakov).

1. Introduction

The Fischer–Tropsch (FT) reaction produces a wide range of hydrocarbons from synthesis gas (mixture of carbon monoxide and hydrogen with a H_2/CO ratio close to 2). The current interest in FT synthesis has been largely driven by the growing demand for clean fuels and rational utilization of natural gas, coal or biomass [1–4]. Industrial FT processes involve cobalt and iron catalysts. Because of their higher productivity and hydrocarbon selectivity at lower temperature and pressure, cobalt supported catalysts have been particularly suitable for the production of middle distillate and hydrocarbon waxes in the low temperature FT process [4–7].

Conventional cobalt FT catalysts are prepared via aqueous impregnation of porous oxide supports with solutions of various salts [4,5,7,8]. After decomposition of supported cobalt salts by drying and calcination, the catalysts are reduced in hydrogen to obtain metallic cobalt, which contains active sites for the reaction. Among the different parameters affecting the catalytic performance, the key factors seem to be cobalt dispersion, reducibility and stability. Indeed, higher concentrations of stable cobalt metal sites typically favor higher FT reaction rates [4–6,7,9,10].

Catalytic support also influences several important properties of cobalt catalysts such as dispersion, reducibility, electronic structure of smaller cobalt particles, diffusion of reagents and reaction products, mechanical and chemical strength [4]. Our previous reports [11–15] have emphasized the impact of the support porous structure on cobalt dispersion in silica supported FT catalysts. Smaller cobalt particles are usually found in narrow pore silicas. It was uncovered [16–19] that the sizes of Co_3O_4 crystallites influenced cobalt reducibility; smaller cobalt oxide particles are known to be more difficult to reduce than larger ones. Similar results have been recently obtained by Holmen et al. [20] for cobalt alumina supported catalysts.

In the case of cobalt alumina supported catalysts, an interaction between cobalt oxide and catalyst support could also result in incorporation of some Al^{3+} ions into Co_3O_4 spinel matrix resulting in $Co^{2+}Co_{2-x}Al_xO_4$ mixed spinels which would hinder the reduction of Co_3O_4 particles [21]. In addition to surface compounds, cobalt alumina supported FT catalysts could also contain bulk cobalt aluminates. Cobalt incorporated in bulk aluminate cannot be reduced by hydrogen in an acceptable temperature range

($T < 773$ K). Hence, the amount of available metallic cobalt for the FT reaction and catalytic activity shrink drastically. Minimization of concentration of hardly reducible mixed cobalt support compounds and optimization of cobalt metal dispersion would therefore result in a better catalytic activity.

The paper addresses the structure and catalytic performance of cobalt Fischer–Tropsch catalysts supported by commercial alumina (Puralox) and silica-doped alumina (Siralox). The effects due to a variation of chemical composition of the support have been investigated separately from the effects which could arise from a different porous support structure. Indeed, alumina and silica-doped alumina supports studied in this work had identical texture. At different stages of the preparation (from aqueous impregnation through calcination and reduction) the catalysts were characterized by X-ray diffraction (XRD), X-ray photoelectron spectroscopy (XPS), and temperature programmed reduction (TPR). The characterization results are discussed together with the results of catalytic evaluation in a fixed bed microreactor.

2. Experimental

Cobalt catalysts were synthesized via incipient wetness impregnation using aqueous solutions of cobalt nitrate. Alumina (Puralox SCCA 5/170, Sasol, pore volume = $0.47\text{ cm}^3\text{ g}^{-1}$, average pore diameter = 80 \AA) and silica-doped alumina (Siralox 5/170, Sasol, 95% Al_2O_3 –5% SiO_2 , pore volume = $0.49\text{ cm}^3\text{ g}^{-1}$, average pore diameter = 83 \AA) were used as catalytic supports. Puralox and Siralox are commercial catalytic supports. Puralox alumina [22] is produced via controlled activation of high purity boehmite. Siralox is prepared by hydrolyzing an aluminum alkoxide, obtained from an alkoxide process [23] at about $90\text{ }^\circ\text{C}$. Thereafter, a dilute solution of orthosilicic acid is added to the stirred mixture. This slurry is then spray-dried. The spray-dried product is calcined to yield Siralox silica-doped alumina [24,25].

The impregnated catalysts were dried at $120\text{ }^\circ\text{C}$ and calcined at $400\text{ }^\circ\text{C}$ in a flow of air (heating ramp $1\text{ }^\circ\text{C}/\text{min}$) and then reduced in hydrogen at $400\text{ }^\circ\text{C}$ with a GHSV = 2000 h^{-1} . The cobalt content in the catalysts was respectively 8 wt.% and 15 wt.%. The catalysts containing 15% of cobalt were prepared in two consecutive impregnations separated by calcination at $400\text{ }^\circ\text{C}$ under airflow. Cobalt content in the catalysts was measured by atomic absorption at the “Service central d’analyse du CNRS” (Vernaison, France). The catalysts are labeled as xCo/S where S designates the

support (Al_2O_3 or $\text{Al}_2\text{O}_3(\text{SiO}_2)$), and x indicates the cobalt content.

The solids were characterized by several characterization techniques. The surface areas were measured by a standard BET procedure using nitrogen adsorption at -196°C on a Micromeritics ASAP 2010 setup. Scanning electron microscopy (SEM) with energy-dispersive X-ray spectroscopy (EDX) was used for morphological and microchemical analysis. The microchemical analysis was performed with a Quanta 200 (FEI) microscope equipped with an EDX microprobe at 5 and 20 keV in order to determine the chemical composition in the interior and at the surface of catalyst grains. The analyses were performed on powder or on a polished slide metalized with carbon. X-ray powder diffraction experiments were conducted using a Bruker AXS D8 diffractometer using $\text{Cu}(\text{K}\alpha)$ radiation for crystalline phase detection. The average crystallite size of Co_3O_4 was calculated using the 511 ($2\theta = 59.5^\circ$) diffraction lines according to the Scherrer equation [26]. The reducibility of the catalysts was studied by temperature programmed reduction (TPR). The TPR was carried out by AutoChem II 2920 apparatus from Micromeritics using 0.5 g of the sample in 5 vol.% H_2/Ar stream ($3.6 \text{ Nl h}^{-1} \text{ g}^{-1}$). The temperature was increased from room temperature to 1000°C at a rate of $2.5^\circ\text{C}/\text{min}$. Surface analyses were performed using a VG ESCA-LAB 220XL X-ray photoelectron spectrometer (XPS). The $\text{Al}_{1\text{ks}}$ non-monochromatized line (1486.6 eV) was used for excitation with a 300 W-applied power. The analyzer was operated in a constant pass energy mode ($E_{\text{pass}} = 40 \text{ eV}$). Binding energies were referenced to the $\text{Al}_{2\text{p}}$ core level (74.6 eV) of the support. The vacuum level during experiments was better than 10^{-7} Pa . The powdered catalyst was pressed as a thin pellet onto a steel block. The reproducibility was $\pm 0.2 \text{ eV}$ for the $\text{Co}2\text{p}$ binding energy.

Carbon monoxide hydrogenation was carried out in a fixed bed stainless steel tubular microreactor ($d_{\text{int}} = 13.1 \text{ mm}$) operating at 20 bars. The catalyst loading was 1 g. The thermocouple was in direct contact with the catalyst. The samples were reduced in hydrogen flow during 10 h at 400°C . After the reduction, the catalyst was cooled down to 190°C and a flow of premixed synthesis gas with a molar ratio $\text{H}_2/\text{CO} = 2$ was gradually introduced to the catalyst. Then, the temperature was slowly increased to 212°C . Gaseous reaction products were analyzed by on-line by gas chromatography. Analysis of H_2 , CO , CO_2 and CH_4 was performed using a packed CTR-1 column and a thermal conductivity detector. Hydrocarbons ($\text{C}_1\text{--}\text{C}_7$) were separated in a capillary Poraplot Q column and analyzed

by a flame-ionization detector. The carbon monoxide contained 5% of nitrogen, which was used as an internal standard for calculating carbon monoxide conversion. The hydrocarbon selectivities were calculated on a carbon basis. Carbon mass balances were respected within the error margin of 10%.

3. Results and discussion

3.1. Cobalt repartition inside and at the surface of the catalyst grains

SEM images of $8\text{Co}/\text{Al}_2\text{O}_3$, $15\text{Co}/\text{Al}_2\text{O}_3$, $8\text{Co}/\text{Al}_2\text{O}_3(\text{SiO}_2)$ and $15\text{Co}/\text{Al}_2\text{O}_3(\text{SiO}_2)$ samples are presented in Fig. 1. The samples mainly contain poly-dispersed spherical particles, with diameter varying from 20 to $160 \mu\text{m}$. The average cobalt content determined by SEM–EDX analysis is in good agreement with the cobalt content determined by X-ray fluorescence (Table 1). This suggests that cobalt repartition is quite uniform at the external surface of the catalyst grains whatever cobalt content and support are used.

In addition, cobalt repartition inside the catalysts was investigated using microtomy; SEM–EDX micrographs of $15\text{Co}/\text{Al}_2\text{O}_3(\text{SiO}_2)$ catalyst have been taken after inclusion in a resin, polishing and metallization in carbon (Fig. 2). EDX analyses have been performed at the shell and in the core of the grain. The Co/Al and Si/Al atomic ratios are displayed in Table 2. The results show that repartitions of cobalt, aluminum and silicon are uniform inside the catalytic grain. The Co/Al and Si/Al atomic ratios obtained in the core or at the shell of the particles are in good agreement with the theoretical atomic ratios.

3.2. Cobalt species in the calcined catalysts

The BET specific surface areas, pore diameters and pore volumes calculated from the isotherms of nitrogen adsorption/desorption on the supports and supported catalysts, are presented in Table 1. The two supports used have almost identical texture. A small decrease in specific surface area and pore volume was observed after cobalt addition in both alumina and silica-doped alumina supported catalysts. This decrease is likely to be attributed to the effect of support “dilution” with cobalt. Indeed, the BET surface areas and pore volume expressed per gram of alumina do not change considerably after modification with cobalt. This indicates that pores of the supports have not been plugged by cobalt species.

The XRD patterns of the calcined catalysts (Fig. 3) represent a combination of peaks attributed to $\gamma\text{-Al}_2\text{O}_3$

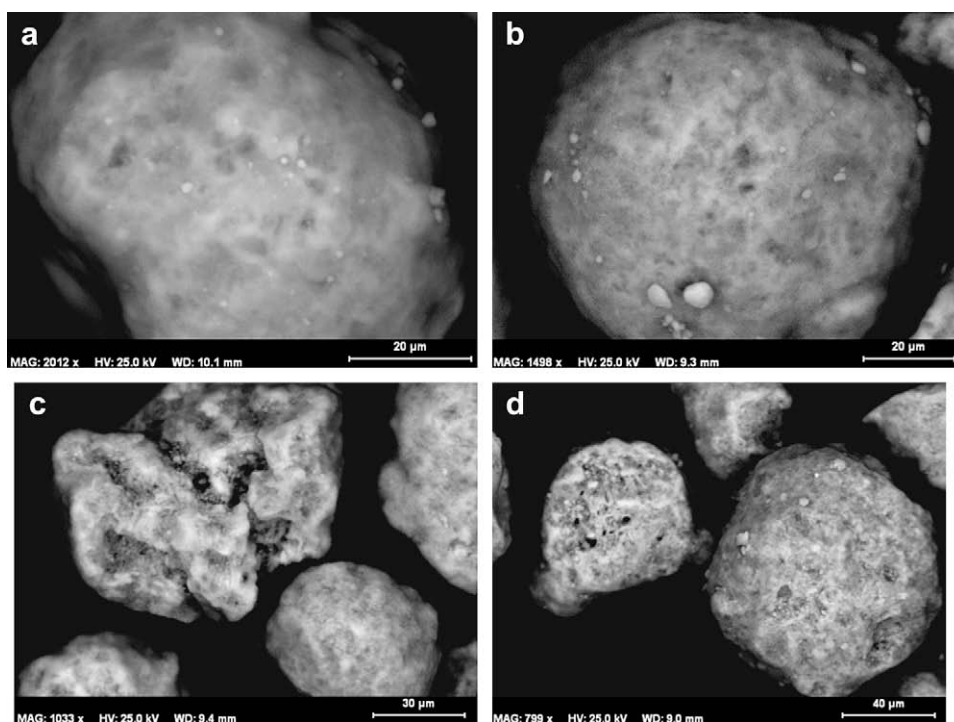


Fig. 1. SEM micrographs of catalysts: a) 8Co/Al₂O₃, b) 8Co/Al₂O₃(SiO₂), c) 15Co/Al₂O₃, d) 15Co/Al₂O₃(SiO₂).

and Co₃O₄ crystalline phases. The diameter of the cobalt oxide crystallites was calculated using the Scherrer equation (Table 1). The average diameter of the cobalt oxide crystallites (around 9 nm) was similar for alumina and silica-doped alumina supported catalysts prepared with 8 wt.% cobalt loading and comparable to the average pore diameter of the two supports (8 nm). This suggests possible dependence of Co₃O₄ particle size on catalyst pore diameter. Indeed, previous reports [11–15,20] uncovered that the sizes of cobalt oxide particles in supported catalysts prepared via aqueous impregnation with cobalt nitrate were principally affected by support pore sizes. The average diameter of the cobalt oxide crystallites slightly increases while increasing cobalt content from 8 to 15 wt.%.

Surface analyses of the calcined samples have been performed by XPS spectroscopy. Co2p XPS spectra of calcined cobalt alumina and cobalt silica alumina supported catalysts (Fig. 4) are indicative of the presence of Co₃O₄ which was identified by the binding energies, peak shape, spin-orbital splitting of 15.2 eV and the absence of intense satellite structure [27–32]. This observation is consistent with XRD data which also hint at the presence of significant Co₃O₄ concentrations in the calcined catalysts. The XPS spectra revealed the presence in the catalysts of aluminum, oxygen and some concentration of residual nitrogen. Note that the XPS concentration of silicon atoms in silica-doped alumina catalysts was relatively low (<1%).

Table 1
Characterization of cobalt supported catalysts.

Sample	Cobalt content (wt.%)	Average Co from SEM (wt.%)	BET surface area (m ² /g)	Average pore diameter (Å)	Total pore volume, (cm ³ /g support)	Size of Co ₃ O ₄ crystallites by XRD (Å)	nCo/nAl ratio from XPS ^a
Al ₂ O ₃	0	0	159	80	0.47	—	—
Al ₂ O ₃ (SiO ₂)	0	0	166	83	0.49	—	—
8Co/Al ₂ O ₃	7.5	8	148	81	0.40	96	0.05
8Co/Al ₂ O ₃ (SiO ₂)	7.6	8.1	143	84	0.41	91	0.05
15Co/Al ₂ O ₃	13.5	15.6	128	79	0.34	124	0.06
15Co/Al ₂ O ₃ (SiO ₂)	13.8	15	126	85	0.36	128	0.06

^a (n_{Co}/n_{Al}) monolayer = 0.08 for 8%Co and 0.18 for 15% Co on either Al₂O₃ or Al₂O₃(SiO₂).

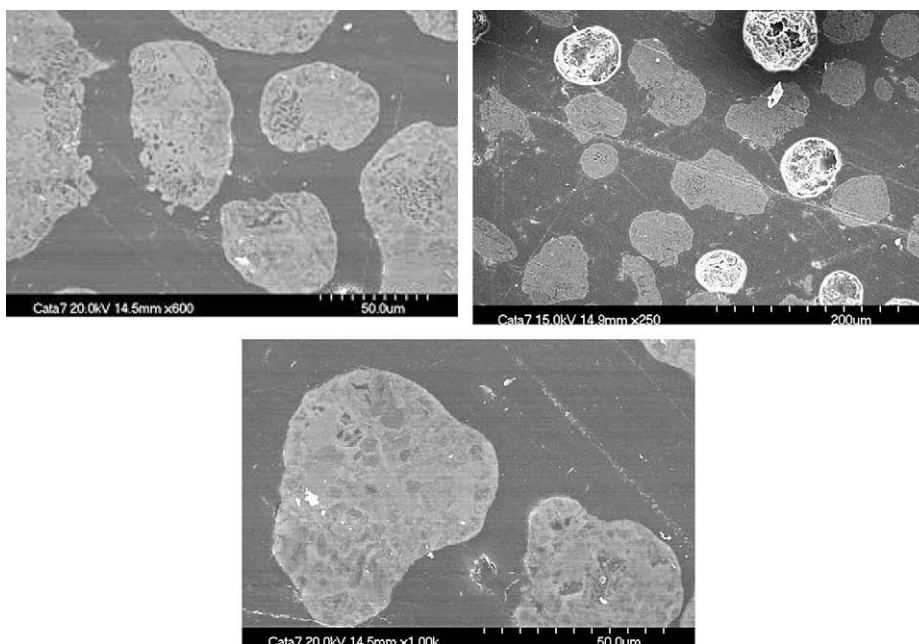


Fig. 2. SEM micrographs taken on polishing slide for 15Co/Al₂O₃(SiO₂) catalyst.

Cobalt dispersion in the calcined catalysts was evaluated by comparing the $n_{\text{Co}}/n_{\text{Al}}$ atomic ratio determined by XPS with the theoretical atomic ratio corresponding to a monolayer coverage of the support by cobalt species [33]. The $n_{\text{Co}}/n_{\text{Al}}$ ratios are rather similar for the two supports (Table 1) which is indicative of comparable cobalt dispersion. This is consistent with the XRD data. Similar cobalt particle size in both catalyst series was calculated using the Scherrer equation from XRD patterns. Note that the $n_{\text{Co}}/n_{\text{Al}}$ atomic ratio determined by XPS does not increase much with cobalt content. This suggests that cobalt introduced in the second impregnation does probably not contribute to the enhancement of surface area of Co₃O₄ crystallites. Moreover, it can be suggested that cobalt introduced in the second impregnation agglomerates on the Co₃O₄ particles which had been formed during the first impregnation step. This suggestion is also consistent with an increase in Co₃O₄ crystallite size observed by XRD after the second impregnation (Table 1).

Fig. 5a and b shows the TPR profiles of 8Co/Al₂O₃, 8Co/Al₂O₃(SiO₂), 15Co/Al₂O₃ and 15Co/Al₂O₃(SiO₂) catalysts. The profiles of these catalysts exhibit three groups of hydrogen consumption peaks: low temperature, medium temperature and high temperature peaks. In agreement with previous reports [21,34,35] the low temperature peaks observed between room temperature and 350 °C were mainly attributed to the reduction of the Co₃O₄ to CoO. The small shoulder at 180 °C seems to be related to the decomposition of residual undecomposed nitrate species in hydrogen [21]. The second group of peaks situated between 350 and 750 °C is mainly attributed to the reduction of CoO particles and cobalt species interacting more strongly with the support to metallic cobalt, while the high temperature peaks ($T > 750$ °C) are probably due to the reduction of cobalt aluminate compounds. The TPR data indicate that doping alumina with silica increases the fraction of easy reducible cobalt oxide phases and results in a significant decrease in the concentration of hardly

Table 2

EDX analyses for 15Co/Al₂O₃(SiO₂) catalyst (Co/Al theoretical ratio = 0.18 and Si/Al theoretical ratio = 0.05).

Type of analysis	Co/Al atomic ratio				Si/Al atomic ratio			
	Average	Standard deviation σ	Min.	Max.	Average	Standard deviation σ	Min.	Max.
Total	0.19	0.01	0.17	0.21	0.06	0.01	0.04	0.06
Core	0.19	0.02	0.15	0.20	0.05	0.01	0.04	0.06
Shell	0.19	0.01	0.17	0.21	0.06	0.01	0.04	0.08

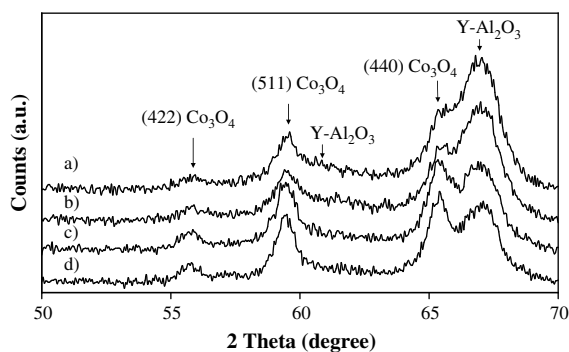


Fig. 3. XRD patterns of calcined catalysts: a) 8Co/Al₂O₃, b) 8Co/Al₂O₃(SiO₂), c) 15Co/Al₂O₃, d) 15Co/Al₂O₃(SiO₂).

reducible cobalt aluminate species (TPR peaks at $T > 750$ °C). Hence, the presence of small amounts of silica (5%) in the alumina support seems to hinder cobalt aluminate formation and enhances cobalt reducibility. Earlier, Barradas et al. [36] showed that coating alumina with a protective layer of silica could protect the catalyst from formation of cobalt aluminate at the conditions of FT synthesis and thus, from loss of the active component during the reaction. Zhang et al. [37] also showed that formation of cobalt aluminate in alumina supported catalysts could be efficiently suppressed by a surface layer of magnesia.

According to the XPS data, in the silica-doped alumina supported catalysts studied, the concentration of Si on the external surface was very low; no enrichment of catalyst surface with SiO₂ was observed. SEM measurements also suggest (Table 2) almost uniform silica repartition in alumina matrix. Thus, lower concentration of cobalt aluminate in cobalt silica-doped alumina supported catalysts cannot be explained in terms of protective layer of silica on alumina. It is known that cobalt aluminate can be

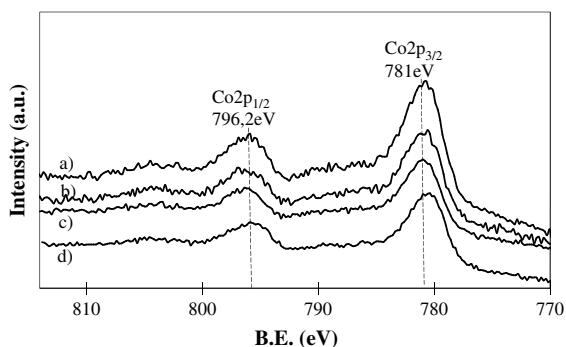


Fig. 4. Co2p XPS spectra of calcined catalysts: a) 8Co/Al₂O₃, b) 8Co/Al₂O₃(SiO₂), c) 15Co/Al₂O₃, d) 15Co/Al₂O₃(SiO₂).

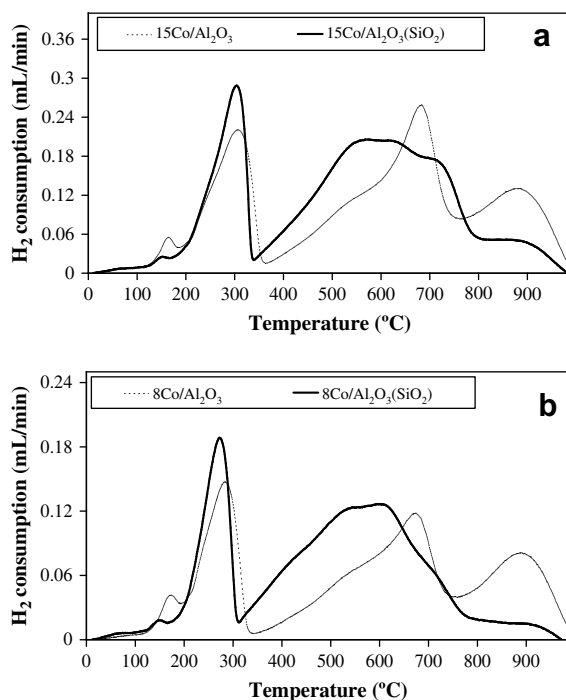


Fig. 5. H₂-TPR profiles of calcined catalysts: a) catalysts with 15 wt.% of cobalt; b) catalysts with 8 wt.% of cobalt.

produced at different stages of catalyst preparation [34,38–40]: cobalt deposition, decomposition of cobalt precursor, catalyst calcination and even reduction. Note that in contrast to Puralox alumina which has a basic character, Siralox silica-doped alumina possesses some acidity, which was recently investigated by Daniell et al. [41]. Previous reports [42–45] suggest that decomposition of cobalt precursors is a crucial step in catalyst preparation which affects the fraction of cobalt-support mixed compounds such as

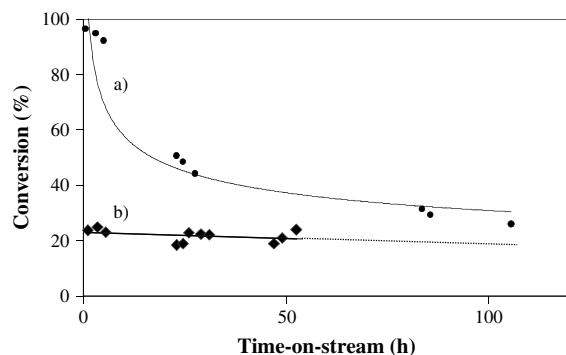


Fig. 6. Catalytic performance of a) 15Co/Al₂O₃ and b) 15Co/Al₂O₃(SiO₂). Experimental conditions: $T = 212$ °C, $P = 20$ bars, GHSV = 5000 h⁻¹.

Table 3
Catalytic performance of cobalt supported catalysts in FT synthesis after 100 h on stream.

Catalyst	Cobalt content (wt.%)	Conversion (%)	S(CH ₄) (%)	S(C ₅₊) (%)
15Co/Al ₂ O ₃	13.5	22	16	77
15Co/Al ₂ O ₃ (SiO ₂)	13.8	26	14	77

cobalt aluminates and cobalt dispersion in the catalysts. Therefore, it can be suggested that lower basicity of Siralox silica-doped alumina relative to Puralox seems to be a factor which could hinder formation of cobalt aluminates at the stage of cobalt precursor decomposition.

3.3. Catalytic results

Fig. 6 displays catalytic performance data obtained for 15Co/Al₂O₃ and 15Co/Al₂O₃(SiO₂) catalysts at 20 bars, 212 °C and GHSV = 5000 h⁻¹. The 15Co/Al₂O₃(SiO₂) catalyst exhibits high initial carbon monoxide conversion, which gradually decreases with time-on-stream. The initial carbon monoxide conversion was much lower with 15Co/Al₂O₃ catalyst (~20%). It stabilizes however, more promptly than with 15Co/Al₂O₃(SiO₂) catalyst. After 100 h of reaction carbon monoxide conversion on both catalysts was between 22 and 26%. At these conditions, the hydrocarbon selectivities were rather similar on both catalysts (Table 3).

The characterization data suggest similar cobalt dispersion in both alumina and silica-doped alumina supported catalysts, while TPR points out a lower concentration of cobalt aluminate and correspondingly better cobalt reducibility in silica-doped alumina than in alumina-supported catalysts. Better reducibility of Co/Al₂O₃(SiO₂) catalysts at similar cobalt dispersion would normally result in higher concentration of cobalt metal sites which are active in FT synthesis. Thus, higher FT catalytic activity of 15Co/Al₂O₃(SiO₂) relative to 15Co/Al₂O₃ catalyst could be possibly attributed to a higher concentration of cobalt metal active sites in these catalysts because of a better reducibility of cobalt.

4. Conclusion

The structure of supported cobalt species in alumina supported catalysts and their catalytic behavior in FT synthesis appear to be strongly affected by doping alumina with small amounts of silica (~5 wt.%). Support and catalyst characterization show that doped

silica has uniform repartition in alumina, no enrichment of alumina subsurface layer by silica was observed. In alumina and silica-doped alumina supported catalysts with similar textural properties, cobalt dispersion was primarily a function of support pore diameter. Higher concentration of hardly reducible cobalt aluminate compounds was detected in cobalt catalysts supported on alumina than in their counterparts supported by alumina doped with silica. The presence of small amounts of silica in alumina supports significantly enhances cobalt reducibility. Higher cobalt reducibility at similar cobalt dispersion seems to be responsible for the higher FT reaction rate on cobalt catalysts supported on silica-doped alumina.

Acknowledgements

The authors thank P. Recourt and N. Djelal for help with the SEM–EDX analyses. IFP is acknowledged for the financial support of this work.

References

- [1] R.B. Anderson, *The Fischer–Tropsch Synthesis*, Academic Press, New York, 1984.
- [2] P. Chaumette, *Revue de l'Institut Français du Pétrole* 51(5) (1996) 711.
- [3] A.C. Vosloo, *Fuel Process. Technol.* 71 (2001) 149.
- [4] A.Y. Khodakov, W. Chu, P. Fongarland, *Chem. Rev.* 107 (2007) 1692.
- [5] M.E. Dry, *Catal. Today* 71 (2002) 227.
- [6] E. Iglesia, S.C. Reyes, R.J. Madon, S.L. Soled, *Adv. Catal.* 39 (1993) 221.
- [7] E. Iglesia, *Appl. Catal.*, A 161 (1997) 59.
- [8] R. Oukaci, A.H. Singleton, J.G. Goodwin, *Appl. Catal.* 186 (1999) 129.
- [9] E. Iglesia, S.L. Soled, R.A. Fiato, *J. Catal.* 137 (1992) 212.
- [10] M. Dry, *Appl. Catal.*, A 138 (1996) 319.
- [11] A.Y. Khodakov, A. Griboval-Constant, R. Bechara, V.L. Zholobenko, *J. Catal.* 206 (2002) 230.
- [12] A.Y. Khodakov, A. Griboval-Constant, R. Bechara, F. Villain, *J. Phys. Chem. B* 105 (2001) 9805.
- [13] A.Y. Khodakov, R. Bechara, A. Griboval-Constant, *Stud. Surf. Sci. Catal.* 142B (2002) 1133.
- [14] A.Y. Khodakov, R. Bechara, A. Griboval-Constant, *Appl. Catal.*, A 254 (2003) 273.
- [15] A. Griboval-Constant, A.Y. Khodakov, R. Bechara, V.L. Zholobenko, *Stud. Surf. Sci. Catal.* 144 (2002) 609.
- [16] H.F.J. van't Blik, R. Prins, *J. Catal.* 97 (1986) 210.
- [17] B. Ernst, A. Bensaddik, L. Hilaire, P. Chaumette, A. Kiennemann, *Catal. Today* 39 (1998) 329.
- [18] D.G. Castner, P.R. Watson, I.Y. Chan, *J. Phys. Chem.* 94 (1990) 819.
- [19] A.Y. Khodakov, J. Lynch, D. Bazin, B. Rebours, N. Zanier, B. Moisson, P. Chaumette, *J. Catal.* 168 (1997) 16.
- [20] S. ØBorgEri, E.A. Blekkan, S. Storsæter, H. Wigum, E. Rytter, A. Holmen, *J. Catal.* 248 (2007) 89.

- [21] W. Chu, P.A. Chernavskii, L. Gengembre, G.A. Pankina, P. Fongarland, A.Y. Khodakov, *J. Catal.* 252 (2007) 215.
- [22] http://www.sasoltechdata.com/tds/PURALOX_CATALOX.pdf.
- [23] G. Albert, M. Kamps, K. Noweck, A. Reichenauer, E. Scherf, U. Ziegler, German patent DE 3244972, 1984, assigned to Condea Chemie.
- [24] A. Meyer, K. Noweck, A. Reichenauer, J. Schimanski, US Patent 5,045,519, 1991, assigned to Condea Chemie.
- [25] P.A. Van Berge, J. Van de Loosdrecht, S. Barradas, US Patent 7,262,225 B2, 2007, assigned to Sasol Technology.
- [26] B.D. Cullity, *Elements of X-Ray Diffraction*, Addison-Wesley, London, 1978.
- [27] T.J. Chaung, C.R. Brundle, D.W. Rice, *Surf. Sci.* 59 (1976) 413.
- [28] J.P. Bonnelle, J. Grimblot, A. D'huysser, *J. Electron. Spectrosc.* 7 (1975) 151.
- [29] M. Oku, Y. Sato, *Appl. Surf. Sci.* 55 (1992) 37.
- [30] D.G. Castner, P.R. Watson, I.Y. Chan, *J. Phys. Chem.* 93 (1989) 3188.
- [31] V.M. Jiménez, A. Fernández, J.P. Espinós, A.R. González-Eliphe, *J. Electron Spectrosc. Relat. Phenom.* 71 (1995) 61.
- [32] J.-G. Kim, D.L. Pugmire, D. Battaglia, M.A. Langell, *Appl. Surf. Sci.* 165 (2000) 70.
- [33] F.P.J. Kerkhof, J.A. Moulijn, *J. Phys. Chem.* 83 (1979) 1612.
- [34] P. Arnoldy, J.A. Moulijn, *J. Catal.* 93 (1985) 38.
- [35] D.I. Enache, M. Roy-Auberger, R. Revel, *Appl. Catal., A* 268 (2004) 51.
- [36] S. Barradas, E.A. Caricato, P.J. van Berge, J. van de Loosdrecht, *Stud. Surf. Sci. Catal.* 143 (2002) 55.
- [37] Y. Zhang, H. Xiong, K. Liew, J. Li, *J. Mol. Catal. A* 237 (2005) 172.
- [38] T. Ataloglou, J. Vakros, K. Bourikas, C. Fountzoula, C. Kordulis, A. Lycourghiotis, *Appl. Catal., B* 57 (2005) 299.
- [39] L.F. Liotta, G. Pantaleo, A. Macaluso, G. Di Carlo, G. Deganello, *Appl. Catal., A* 245 (2003) 167.
- [40] B. Jongsomjit, J. Panpranot, J.G. Googwin, *J. Catal.* 204 (2001) 98.
- [41] W. Daniell, U. Schubert, R. Glöcker, A. Meyer, K. Noweck, H. Knözinger, *Appl. Catal., A* 196 (2000) 247.
- [42] J. van de Loosdrecht, S. Barradas, E.A. Caricato, N.G. Ngwenya, P.S. Nkwanyana, M.A.S. Rawat, B.H. Sigwebela, P.J. van Berge, J.L. Visagie, *Top. Catal.* 26 (2003) 121.
- [43] J.R.A. Sietsma, J.D. Meeldijk, J.P. den Breejen, M. Versluijs-Helder, A.J. van Dillen, P.E. de Jongh, K.P. de Jong, *Angew. Chem. Int. Ed.* 46 (2007) 4547.
- [44] W. Chu, L.-N. Wang, P.A. Chernavskii, A.Y. Khodakov, *Angew. Chem. Int. Ed.* 47 (2008) 5052.
- [45] J.-S. Girardon, E. Quinet, A. Griboval-Constant, P.A. Chernavskii, L. Gengembre, A.Y. Khodakov, *J. Catal.* 248 (2007) 143.